Metallurgical Aspects of Fatigue Failure of Steel-Part I

Dr. Ahmed Sharif
Department of Materials and Metallurgical Engineering
Bangladesh University of Engineering and Technology

Biography

Dr. Ahmed Sharif received his first class honours B.Sc. Engineering degree in Metallurgical Engineering from the Bangladesh University of Engineering and Technology (BUET), Dhaka in 1998 and also the M. Sc. Engineering degree in 2001. He began his academic career with the same department as a Lecturer from 1999 and was promoted to Associate Professor in 2010. He completed his Ph. D. in 2005 from City University of Hong Kong (CityU). His electronic packaging materials research, has led to the award of an international prize the "IEEE CPMT Young Scientist Award" from IEEE Japan chapter in 2004. His publication record, 40 peer-reviewed (SCI listed) journal papers with h-index of 17 reflects his potentiality and leadership qualities in research.

Metallurgical Aspects of Fatigue Failure of Steel-Part I

Dr. Ahmed Sharif
Department of Materials and Metallurgical Engineering
Bangladesh University of Engineering and Technology

ABSTRACT

Metals when subjected to repeated cyclic loadexhibit damage by fatigue. The magnitude of stress in each cycle is not sufficient to cause failure with a single cycle. Large numbers of cycles are therefore needed for failure by fatigue. Importantly, fatigue crack nucleates and grows at stress levels far below the monotonic tensile strength of the metal. The crack advances continuously by very small amounts, its growth rate decided by the magnitude of load and geometry of the component. There has been much research into fatigue of steel. In this context, at first the major microstructures and the phase transformations by which these microstructures in carbon and low-alloy steels are developed are described briefly. Later on, some knowledge of basic aspects of the fatigue mechanism is described with particular emphasis on the developments in fatigue life prediction methods.

1.1 Introduction to Steel

The term steel is used for many different alloys of iron. These alloys vary both in the way they are made and in the proportions of the materials added to the iron. All steels, however, contain small amounts of carbon and manganese. In other words, it can be said that steel is a crystalline alloy of iron, carbon and several other elements, which hardens above its critical temperature. Steel, by definition, must be at least 50% Fe and must contain one or more alloying element. These alloying elements include carbon, manganese, silicon, nickel, chromium, molybdenum, phosphorus, copper, vanadium, titanium, niobium, boron, and aluminum. Carbon steels, generally called plain carbon steels, range in carbon content from approximately 0.10% C to over 1% C.

1.2 Classification of Steels

Steels can be classified by a variety of different systems depending on:

- The composition, such as carbon, low-alloy, or stainless steels
- The manufacturing methods, such as open hearth, basic oxygen process, or electric furnace methods
- The finishing method, such as hot rolling or cold rolling
- The product form, such as bar, plate, sheet, strip, tubing, or structural shape
- The deoxidation practice, such as killed, semikilled, capped, or rimmed steel
- The microstructure, such as ferritic, pearlitic, and martensitic
- The heat treatment, such as annealing, quenching and tempering, and thermomechanical processing

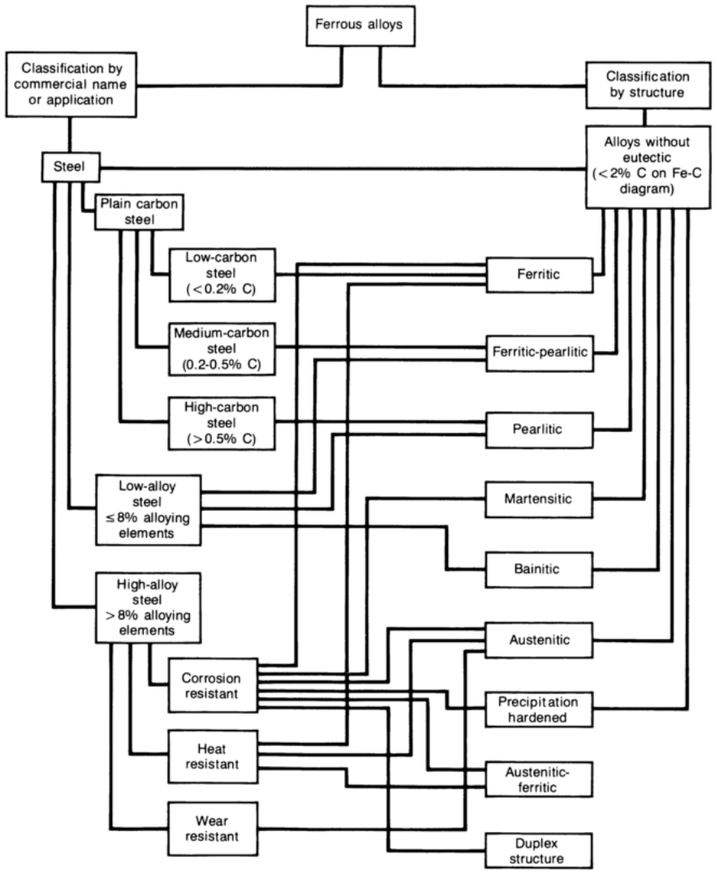

Fig. 1 Classification of steels. Source: D.M. Stefanescu, University of Alabama,TuscaloosaOf the aforementioned classification systems, chemical composition is the most widely used internationally and will be emphasized in this article.

1.3 The EquilibriumDiagram

A phase diagram is a graphical representation of the microstructural changes in relation to composition, and temperature in an alloy system. For steel, the system is called as the iron-carbon diagram.By reference to the diagram, structural or physical condition can be found exactly at any given temperature for steel of any composition in the series. We can also in many cases forecast with a fair degree of accuracy the effect of a particular heat-treatment on the alloy. These are two of the more important uses of the thermal-equilibrium diagram as a metallurgical tool. Plain carbon steels are generally defined as being those alloys of iron and carbon which contain up to 2.0% carbon.

Iron, at temperatures below 910°C, has a body-centred cubic structure (Fig. 2), and above this temperature the structure will change to facecentred cubic (Fig. 3). On cooling, the change is reversed and a body-centred cubic structure is once more formed. The importance of this reversible transformation lies in the fact that up to 2.0% carbon can dissolve in face-centred cubic iron, forming what is known as a 'solid solution', whilst in body-centred cubic iron no more than 0.02% carbon can dissolve in this way.As a piece of steel in its face-centred cubic form cools slowly and changes to its bodycentred cubic form, any dissolved carbon present in excess of 0.02% will be precipitated, whilst if it is cooled rapidly enough such precipitation is prevented.

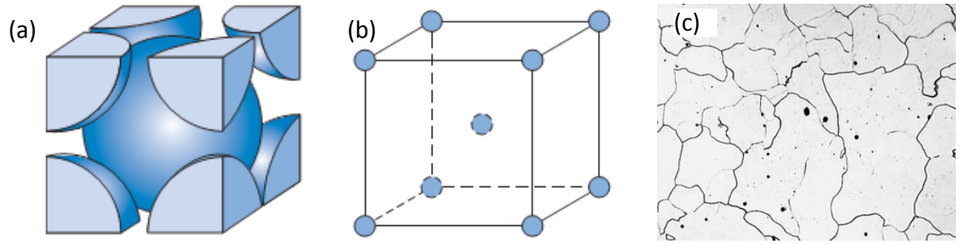

Fig.2 For the body centered cubic crystal structure, (a) a hard sphere unit cell representation, (b) a reduced-sphere unit cell, and (c) photomicrograph of ferrite.

The solid solution formed when carbon atoms are absorbed into the face-centred cubic structure of iron is called Austeniteand the extremely low level of solid solution formed when carbon dissolves in body-centred cubic iron is called Ferrite. For many practical purposes we can regard ferrite as having the same properties as pure iron. The symbol ɣ('gamma') is used to denote both the face-centred cubic form of iron and the solid solution austenite, whilst the symbol (α'alpha') is used to denote both the body-centred cubic form of iron existing below 910°C and the solid-solution ferrite.

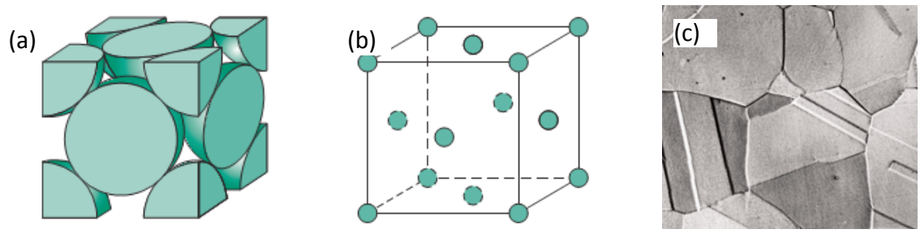

Fig. 3 For the facecentered cubic crystal structure,

(a) a hard sphere unit cell representation, (b) a reduced-sphere unit cell, and (c) photomicrograph of austenite

When carbon is precipitated from austenite it is not in the form of elemental carbon (graphite), but as the compound iron carbide, Fe_3C, usually called Cementite(Fig. 4). This substance, like most other metallic carbides, is very hard, so that, as the amount of carbon (and hence, of cementite) increases, the hardness of the slowly cooled steel will also increase.

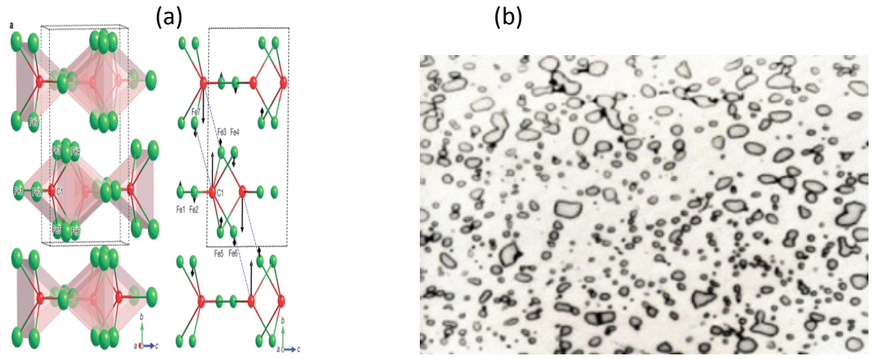

Fig.4 (a) Crystal structure of cementite (green and red spheres represent Fe and C atoms, respectively) and (b) spheroidite microstructures of steel. The light regions are ferrite while the dark are cementite.

Pearliteis another common constituent in plain carbon and low-alloy steels and consists of two phases: ferrite and cementite. The ferrite and cementite phases form a platelike lamellar morphology. The pearlite appears dark in these microstructures, because the etchant attacked the ferrite phase in the pearlite, leaving the cementite phase untouched. Many colonies of pearlite are shown in this micrograph (Fig. 5). A colony represents a single orientation of the pearlite lamella. In these heavily etched specimens, the cementite plates are evident, because the ferrite between the plates has been dissolved by the etching solution.

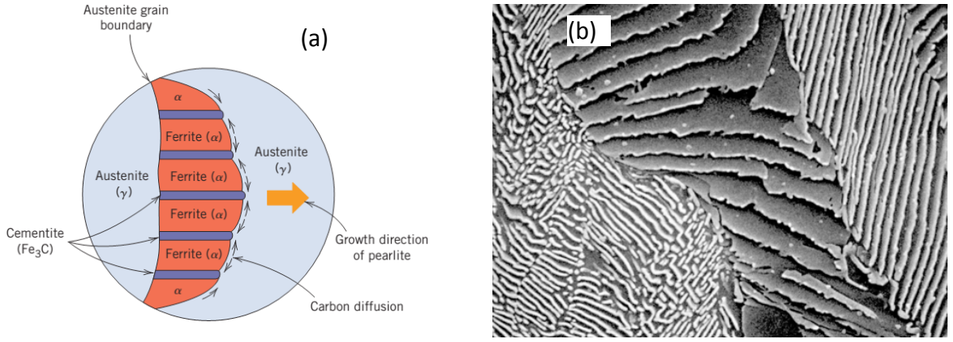

Fig. 5 (a) Schematic representation of the formation of pearlite from austenite;
direction of carbon diffusion indicated by arrows and
(b) Microstructure of pearlite colonies in plain carbon UNS G10800 steel
taken in the scanning electron microscope.

Bainiteis also a constituent that consists of two phases: ferrite and cementite. The appearance of bainite (Fig. 6), which forms at much faster cooling rates than pearlite, is totally different than pearlite. Unfortunately, bainite can have vastly different morphologies. Classic bainites are called either upper bainite or lower bainite, because they form at higher (upper bainite) or lower (lower bainite) temperatures during transformation from austenite. Bainite, if viewed at high magnification, will appear as needles or laths of ferrite, with carbides at the lath boundaries (upper bainite) or within the laths themselves (lower bainite).

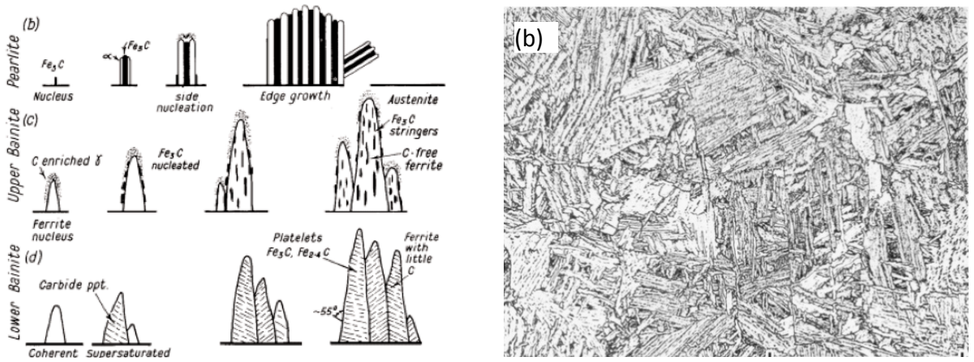

Fig. 6(a) Schematic representation of the formation of (a) peartlite, (b) upper bainite, (c) lower bainite from austenite and (d) microstructure of heat treated low-alloy steel showing bainite. 4% picral + 2% nital etch.

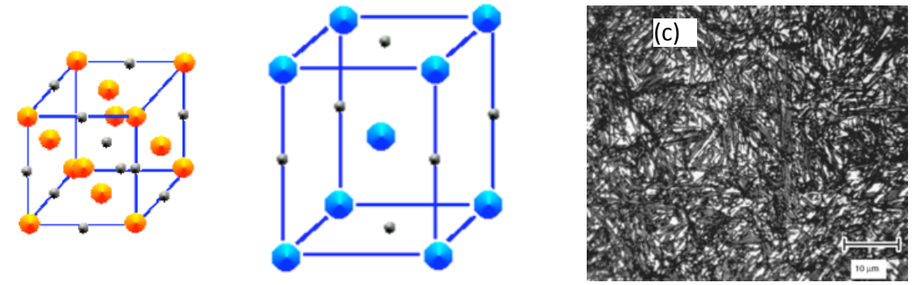

Martensiteis a constituent that is formed by rapid cooling (quenching) plain carbon or low-alloy steels from the high-temperature austenite phase (Fig. 7). Carbon is dissolved in the ferrite well past its room-temperature solubility limit of 0.005% C, and thus, the constituent is no longer considered ferrite. Because of the supersaturated carbon, martensite is a very hard constituent. To be useful, martensite is usually tempered (heated to a temperature between approximately 420 and 650°C, or 800 and 1200°F) to allow some of the carbon to precipitate out as a carbide phase, usually cementite.

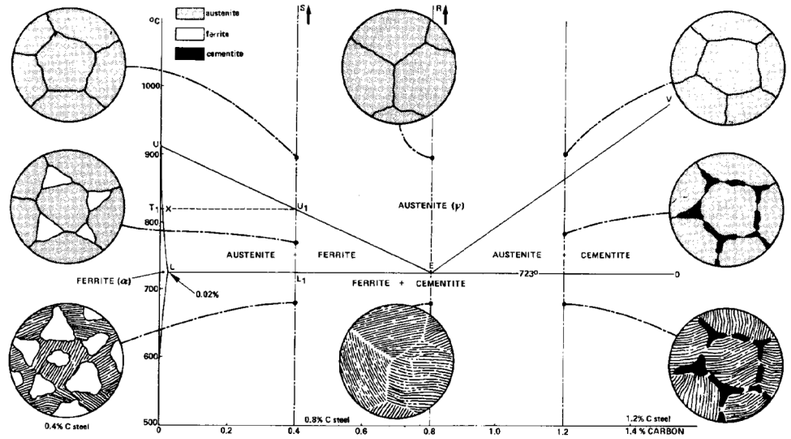

Fig. 7(a) Crystal structure of austenite and martensite (green and red spheres represent Fe and C atoms, respectively)
(b) microstructure of water-quenched low-alloy steel showing plate martensite.

Fig.8 shows us the temperatures at which transformation begins and ends for any solid plain carbon steel. The allotropic transformation temperature of face-centred cubic iron is altered by adding carbon. Figure 7 includes only a part of the whole iron-carbon equilibrium diagram, but it is the section which we make use of in the heat-treatment of carbon steels. On the extreme left of this diagram is an area labeled ‘ferrite’. This indicates the range of temperatures and compositions over which carbon can dissolve in body-centred cubic iron. Temperature governs the degree of solubility of solids in liquids in exactly the same way.

If a steel containing 0.40% carbon is heated to some temperature above U_1 it will become completely austenitic (Fig 8). On cooling, again to just below U_1 (which is called the 'upper critical temperature' of the steel), the structure begins to change from one which is face-centred cubic to one which is body centred cubic. Consequently, small crystals of body-centred cubic iron begin to separate out from the austenite. These body-centred cubic ferrite crystals retain a small amount of carbon (less than 0.02%). As the temperature continues to fall the crystals of ferrite grow in size at the expense of the austenite, and since ferrite is almost pure iron, it follows that most of the carbon present accumulates in the shrinking crystals of austenite. As the temperature falls still farther, the carbon begins to precipitate as cementite. At the same time ferrite is still separating out and we find that these two substances, ferrite and cementite, form as alternate layers of pearlite until all the remaining austenite is used up.

Any steel containing less than 0.8% carbon will transform from austenite to a mixture of ferrite and pearlite in a similar way when cooled from its austenitic state. Transformation will begin at the appropriate upper critical temperature (given by a point on CE which corresponds with the composition of the steel) and end at the lower critical temperature of 723°C. The relative amounts of ferrite and pearlite will depend upon the carbon content of the steel (Fig 8), but in every case the ferrite will be almost pure iron and the pearlite will contain exactly 0.8% carbon. A steel containing 0.8% carbon will not begin to transform from austenite on cooling until the point E is reached. Then transformation will begin and end at the same temperature (723°C). Since the steel under consideration contained 0.8% carbon initially, it follows that the final structure will be entirely pearlite. Any steel containing more than 0.8% carbon will have a structure consisting of cementite and pearlite if it is allowed to cool slowly from its austenitic state.

1.4 General Properties of Plain Carbon Steel

Carbon steel is by far the most widely used kind of steel. Carbon steel is made into a wide range of products, including structural beams, car bodies, kitchen appliances, and cans. In fact, there are 3 types of plain carbon steel and they are low carbon steel, medium carbon steel, high carbon steel, and as their names suggests all these types of plain carbon steel differs in the amount of carbon they contain. The properties of carbon steel depend primarily on the amount of carbon it contains. Indeed, it is good to precise that plain carbon steel is a type of steel having a maximum carbon content of 1.5% along with small percentages of silica, sulphur, phosphorus and manganese. Generally, with an increase in the carbon content from 0.01 to 1.5% in the alloy, its strength and hardness increases but still such an increase beyond 1.5% causes appreciable reduction in the ductility and malleability of the steel.

Low carbon steel or mild steel, containing carbon up to 0.25% responds to heat treatment as improvement in the ductility is concerned but has no effect in respect of its strength properties.Medium carbon steels, having carbon content ranging from 0.25 to 0.70% improves in the machinability by heat treatment. High carbon steels contain carbon in the range of 0.70 to 1.05%. In the fully heat-treated condition it is very hard and it will withstand high shear and wear and will thus be subjected to little deformation. Moreover, at maximum hardness, the steel is brittle and if some toughness is desired it must be obtained at the expense of hardness. Other properties of plain carbon steel are illustrated in Table 1.

Table 1Physical properties of plain carbon steel

Material	Density 10^3 kgm^{-3}	Thermal conductivity $Jm^{-1}K^{-1}s^{-1}$	Thermal expansion $10^{-6}K^{-1}$	Young's modulus GNm^{-2}	Tensile strength MNm^{-2}	% Elongation
0.2% C Steel	7.86	50	11.7	210	350	30
0.4% C Steel	7.85	48	11.3	210	600	20
0.8% C Steel	7.84	46	10.8	210	800	8

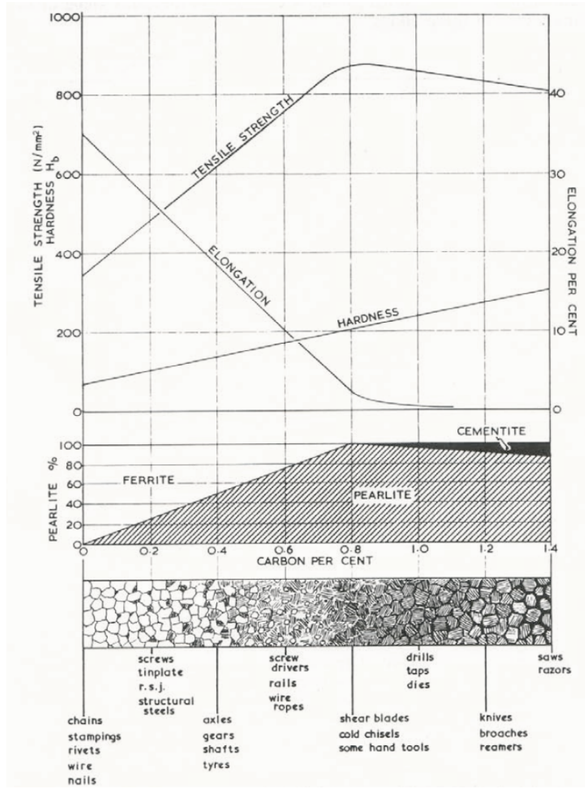

Fig. 9 Diagram showing the relationship between carbon content, microstructure and mechanical properties of plain carbon steels in thenormalized condition.

1.5 The Uses of Plain Carbon Steels

As shown in Fig.9, the hardness of a plain carbon steel increases progressively with increase in carbon content, so that generally the low and medium-carbon steels are used for structural and constructional work, whilst the high-carbon steels are used for the manufacture of tools and other components where hardness and wear-resistance are necessary. Fig.10shows hardness as a function of carbon content for various types of microstructures. Although the hardness-carbon relationships are shown as lines inFig. 10, they are in fact better represented as bands because many factors may cause variations in hardness in a given microstructure. For example, the strength of low-carbon ferritic microstructures is very sensitive to grain size, while that of largely pearlitic microstructures is very sensitive to the interlamellar spacing of cementite and ferrite.

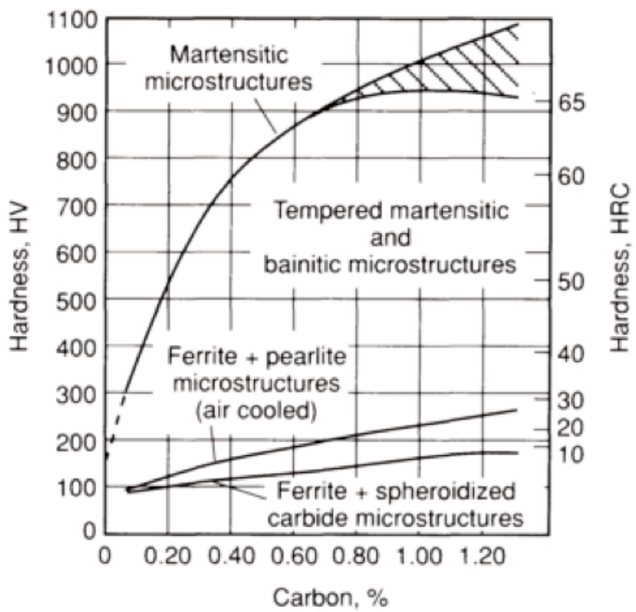

Fig. 10 Hardness as a function of carbon content for various microstructures in steels.

Crosshatched area shows effect of retained austenite.

All types of microstructures increase in strength with increasing carbon content, but martensitic microstructures show the most dramatic increases. Because of the low solubility of carbon in ferrite (except for as-quenched martensite), the carbon is primarily concentrated in carbide phases. Therefore, much of the higher strength of medium- and high-carbon steels is due to higher volume fractions and finer dispersions of carbides in ferrite. Ferritic matrix grain sizes and morphology also significantly affect mechanical behavior at any given carbon level.Fig.10shows that all types of microstructures could be produced in a steel of a given carbon con tent.

2. Overview of Mechanical Characterization of Materials

The structural materials in service are subjected to loads, or forces. In such real conditions it is necessary to know the mechanical properties of the materials in order to avoid excessive deformation and fracture of a structural component. To assure performance, safety and durability of machines, vehicles, nuclear reactors and any structure in general, it is necessary to prevent excessive deformation of their component parts, and also, cracking that can progress up to produce the complete fracture of the parts must be entirely avoided, or strictly limited. The mechanical properties of materials are determined by performing carefully laboratory experiments and measurements under conditions similar to the service conditions of the particular material. This is the mechanical testing of materials. The mechanical characterization of materials, i.e. the study of their deformation and cracking, is the mean by which the behavior of a structural material in service can be predicted. The knowledge of the mechanical characteristics or properties of materials provides the basis for preventing failure of materials in service. Once the mechanical properties of a material are quantitatively determined from mechanical tests, its chances of success in a particular structural application can be evaluated. The most basic criterion in design to avoid structural failure is that the applied stress in a component must not go above the threshold stress that produces the failure of the material. It is named strength of the material. When the material failure produces cracking to an extension that a component is separated into two or more pieces, it is named fracture. If the material sample changes in shape or size, the failure is termed deformation. Deformation and fracture present different types of failure according to the causes and mechanisms. The basic types of material failure corresponding to deformation and fracture are given in Fig. 11.

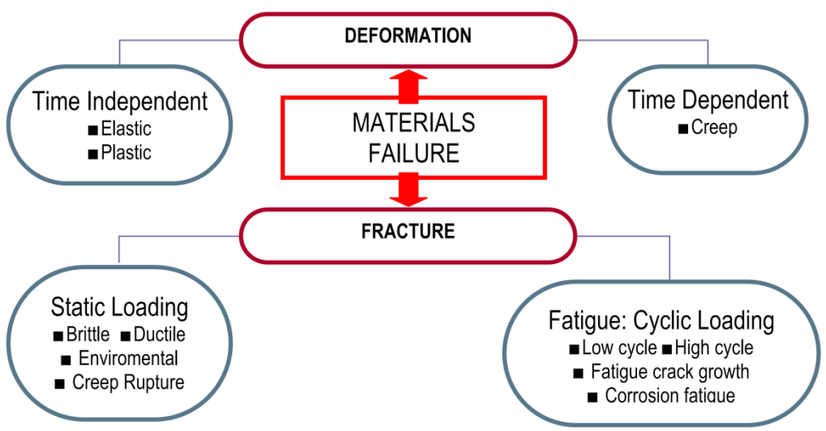

Fig. 11 Schematic representation of the basic types of material failure corresponding to deformation and fracture

2.1 Static loading

When a sufficient load is applied to a metal or other structural material, it will cause the material to change shape. This change in shape is called deformation. A temporary shape change that is self-reversing after the force is removed, so that the object returns to its original shape, is called elastic deformation. In other words, elastic deformation is a change in shape of a material at low stress that is recoverable after the stress is removed. This type of deformation involves stretching of the bonds, but the atoms do not slip past each other.

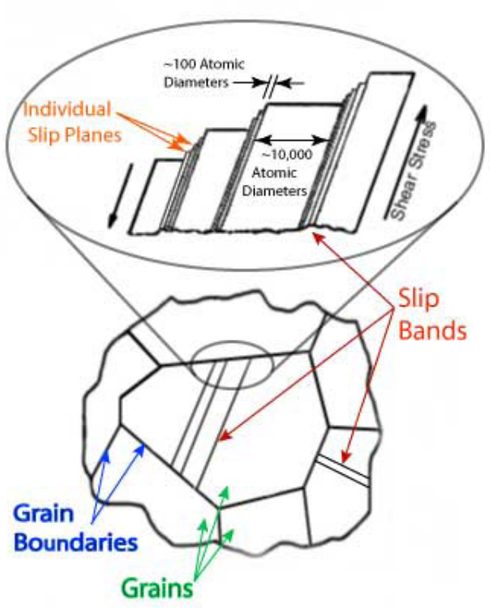

Fig. 12 Schematic representation of deformation of polycrystalline material through slip planes.

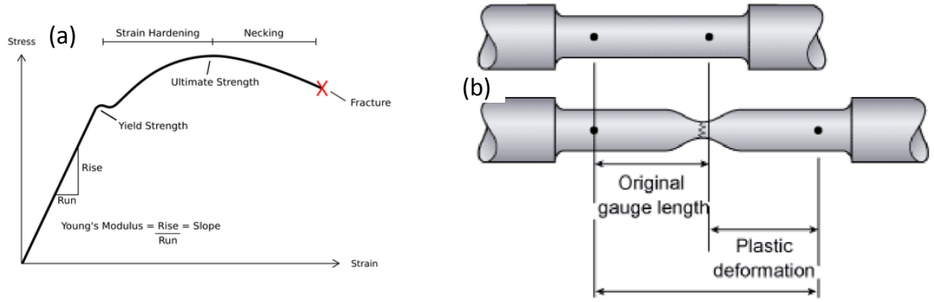

Fig. 13 (a) Typical stress vs. strain diagram with the various stages of deformation and (b) standard tensile specimen before and after tensile test.

When the stress is sufficient to permanently deform the metal, it is called plastic deformation. Plastic deformation involves the breaking of a limited number of atomic bonds by the movement of dislocations. The force needed to break the bonds of all the atoms in a crystal plane all at once is very great. However, the movement of dislocations allows atoms in crystal planes to slip past one another at a much lower stress levels. Since the energy required to move is lowest along the densest planes of atoms, dislocations have a preferred direction of travel within a grain of the material. This results in slip that occurs along parallel planes within the grain. These parallel slip planes group together to form slip bands, which can be seen with an optical microscope. A slip band appears as a single line under the microscope, but it is in fact made up of closely spaced parallel slip planes as shown in the image (Fig. 12). Under tensile stress, plastic deformation is characterized by a strain hardening region and a necking region and finally, fracture (also called rupture) (Fig. 13). During strain hardening the material becomes stronger through the movement of atomic dislocations. The necking phase is indicated by a reduction in cross-sectional area of the specimen. Necking begins after the ultimate strength is reached. During necking, the material can no longer withstand the maximum stress and the strain in the specimen rapidly increases. Plastic deformation ends with the fracture of the material.

2.2 Cyclic loading

2.2.1 Behavior of materials under cyclic loading

The mechanical response of a material is substantially altered by cyclic loadings. In the case of metals, it depends greatly upon hardness of materials and experimental conditions. Under cyclic loading conditions, a metal may harden, soften, remain stable, or have mix behavior (soften or harden depending upon strain level). During constant strain cycling of a material, an increase in stress with time is called strain hardening and a decrease in stress is called a strain softening. These are related to the nature and stability of the dislocation substructure of a given metallic material. In general, the dislocation density is low for soft materials. For such a material, the increase in the density resulting from cyclic plastic straining causes strain hardening. Whereas for a hard metal, the cyclic strain causes a rearrangement of dislocations. The resulting structure for the metal becomes soft as it offers low resistance to deformation. Fluctuating loads are more dangerous than monotonic loads.

2.2.2 Cyclic vs Static Loading

Table 2 Key difference between static and cyclic loading

Static loading	Cyclic loading
Until applied stress intensity factor (K) reaches critical stress intensity factor (Kc) (30 MPa √m for example) the crack will not grow.	K applied can be well below Kc (3 MPa √m for example). Over time, the crack grows.

Key difference between static and cyclic loading are shown Table 2. The design may be safe considering static loads, but any cyclic loads must also be considered.

2.2.3 Typical example on the effect of cyclic loading

In the Aloha Airlines incident on April 28, 1988, an aircraft operated within the manufacturer's guidelines suffered a catastrophic failure (Fig. 14). In this case, the aircraft was subjected to a large number of very short flight cycles and consequently a large number of pressurization cycles for relatively few airframe hours- the end user was flying a very frequent hopping service between Hawaiian Islands. This was also predominantly at a relatively low flight level where there was quite a lot of salt water vapor present. The consequence was that the fuselage failed due

to fatigue along rows of rivet holes - stress concentrators. Fortunately, few people died (1?), and so this is a good example of the necessity to understand fatigue properly even when simply operating aircraft, in that the normal life and inspection interval rules are made with some flight profile assumptions in mind and if you are using the product outside of those assumptions, then you may need to check that they are correct.

Fig. 14 Aircraft after landing in the Aloha airlines incident. After 89,090 flight cycles on a 737-200, metal fatigue lets the top go in flight.

3 Fatigue

3.1 Introduction to fatigue

Fatigue failures in metallic structures are a well-known technical problem. Already in the 19th century several serious fatigue failures were reported and the first laboratory investigations were carried out. Noteworthy research on fatigue was done by August Wöhler. He recognized that a single load application, far below the static strength of a structure, did not do any damage to the structure. But if the same load was repeated many times it could induce a complete failure. In the 19th century fatigue was thought to be a mysterious phenomenon in the material because fatigue damage could not be seen. Failure apparently occurred without any previous warning. The history of engineering structures until now has been marked by numerous fatigue failures of machinery, moving vehicles, welded structures, aircraft, etc. From time to time such failures have caused catastrophic accidents, such as an explosion of a pressure vessel, a collapse of a bridge, or another complete failure of a large structure. Many fatigue problems did not reach the headlines of the newspapers but the economic impact of non-catastrophic fatigue failures has been tremendous. Fatigue of structures is now generally recognized as a significant problem.

3.2 Fatigue as a phenomenon in the material

In a specimen subjected to a cyclic load, a fatigue crack nucleus can be initiated on a microscopically small scale, followed by crack grows to a macroscopic size, and finally to specimen failure in the last cycle of the fatigue life (Fig. 15). The fatigue failure occurs after three different stages, namely:

1. Crack initiation at points of stress concentration

2. Crack growth

3. Final rupture

(a)

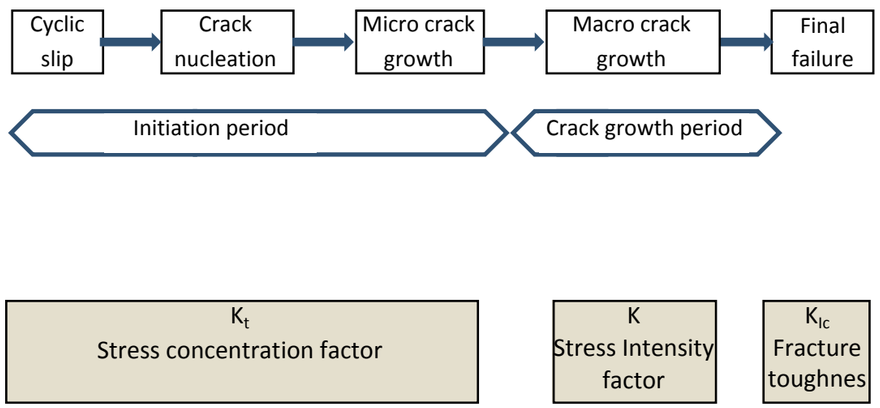

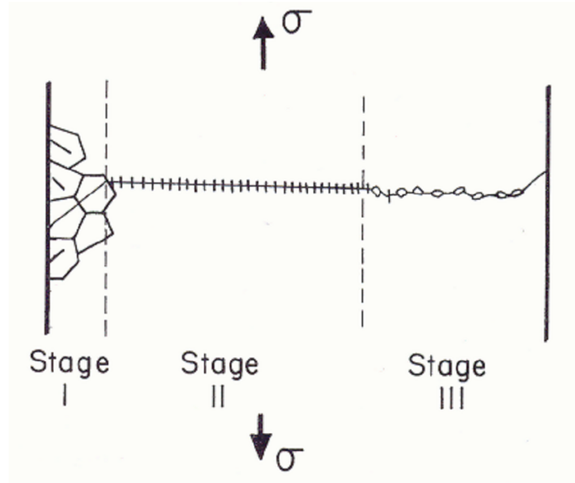

(b)

Fig. 15 (a) Different phases of the fatigue life and relevant factors and (b) schematic drawing of the fatigue crack propagation.

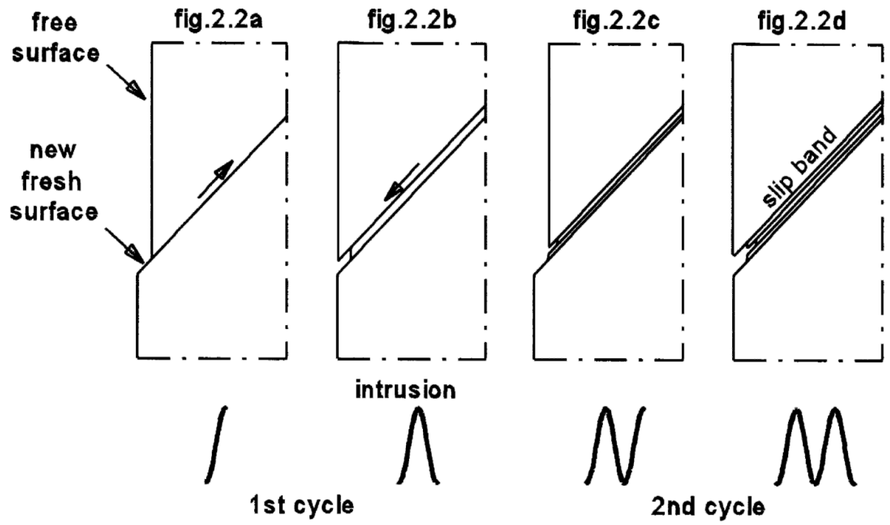

Fig. 16 Cycle slip leads to crack nucleation.

3.2.1 Crack initiation

Fatigue occurs at stress amplitudes below the yield stress. At such a low stress level, plastic deformation is limited to a small number of grains of the material. This microplasticity preferably occurs in grains at the material surface because of the lower constraint on slip. On a microscale

the shear stress is not homogeneously distributed through the material. In some grains at the material surface, these conditions are more favorable for cyclic slip than in other surface grains. If slip occurs in a grain, a slip step will be created at the material surface (Fig.16a). A slip step implies that a rim of new material will be exposed to the environment. The fresh

surface material will be immediately covered by an oxide layer in most environments, at least for most structural materials. Such monolayers strongly adhere to the material surface and are not easily removed. Another significant aspect is that slip during the increase of the load also implies some strain hardening in the slip band. As a consequence, upon unloading (Fig.16b) a larger shear stress will be present on the same slip band, but now in the reversed direction. The same sequence of events can occur in the second cycle, see Fig.16c and d.

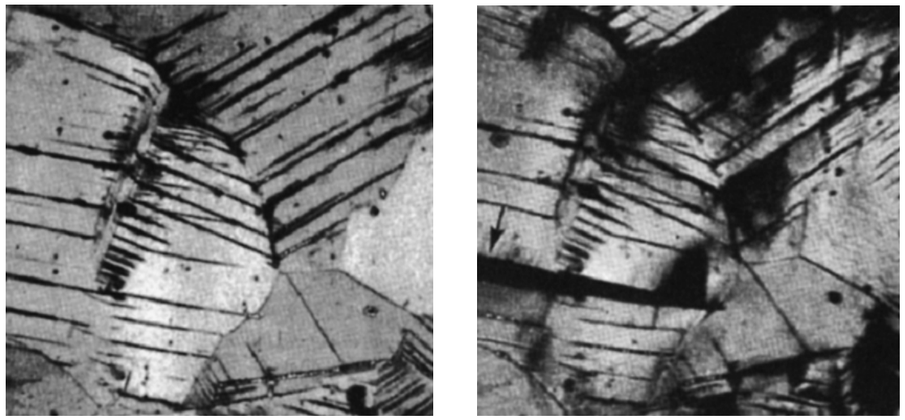

(a) Slip lines are clearly visible

(b) Same as in (a) but plastically strained (5%) which opens a microcrack, see arrow

Fig. 17 Development of cyclic slip bands and a microcrack in a pure copper specimen.

Not all fatigue cracks nucleate along slip bands although in many cases slip bands are at least indirectly responsible for microcracks initiating in metals (Fig. 17). Under fatigue loading conditions, fatigue cracks may nucleate at or near material discontinuities. Discontinuities include inclusions, second-phase particles, corrosion pits, grain boundaries, twin boundaries, pores, voids, and also slip bands. Microcracks in high strength or brittle behaving metals are often formed directly at inclusions or voids, and then grow along planes of maximum tensile stresses.

3.2.2 Crack growth

As long as the size of the microcrack is still in the order of a single grain, the microcrack is obviously present in an elastically anisotropic material with a crystalline structure and a number of different slip systems. The microcrack contributes to an inhomogeneous stress distribution on a microlevel, with a stress concentration at the tip of the microcrack. As a result, more than one slip system may be activated. Moreover, if the crack is growing into the material in some adjacent grains, the constraint on slip displacements will increase due to the presence of the neighbouring grains. Similarly, it will become increasingly difficult to accommodate the slip displacements by slip on one slip plane only. It should occur on more slip planes. The microcrack growth direction will then deviate from the initial slip band orientation. In general, there is a tendency to grow perpendicular to the loading direction, see Fig.18.

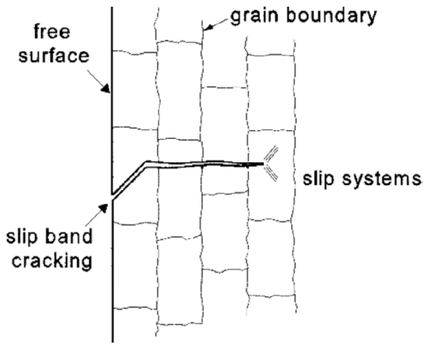

Fig. 18 Cross section of a microcrack during fatigue.

Most fatigue cracks grow across grain boundaries (transcrystalline) or along grain boundaries (intercrystalline) depending on the material, load, and environmental conditions (Fig. 19).

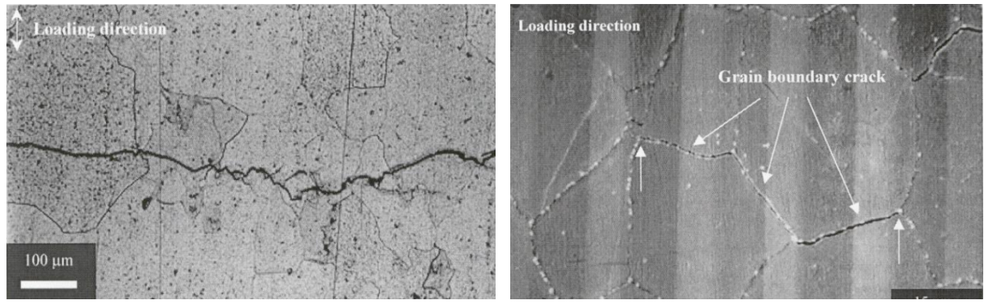

Fig. 19 Scanning electron micrographs showing (a) transcrystalline and (b) intercrystalline fatigue cracks.

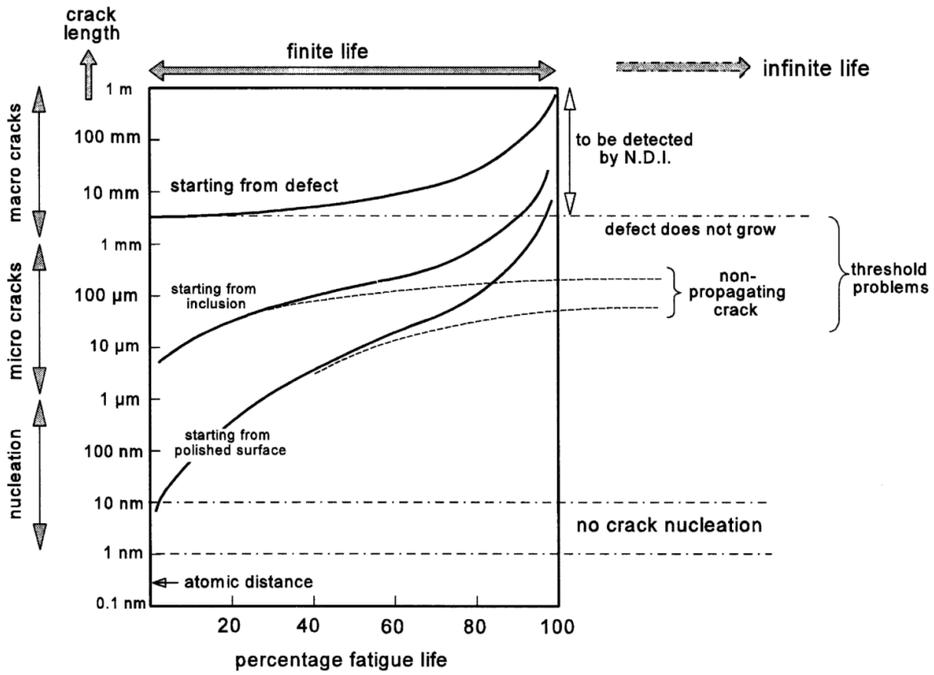

Fig. 20 Different scenarios of fatigue crack growth.

The crack initiation period includes the initial microcrack growth. Because the growth rate is still low, the initiation period may cover a significant part of the fatigue life. This is illustrated by the generalized picture of crack growth curves presented in Fig.20 which schematically shows the crack growth development as a function of the percentage of the fatigue life consumed (=n/N), with nas the number of fatigue cycles and Nas the fatigue life until failure. Complete failure corresponds to n/N=1=100%. There are three curves in Fig.20, all of them in agreement with crack initiation in the very beginning of the fatigue life, however, with different values of the initial crack length. The lower curve corresponds to microcrack initiation at a “perfect” surface of the material. The middle curve represents crack initiation from an inclusion.

The upper curve is associated with a crack starting from a material defect which should not have been present, such as defects in a welded joint.

3.2.3 Final fracture

Cracks will continue to grow if tensile stresses are high enough and at some point, the crack becomes so large that sudden failure occurs. Patterns can be seen on the fracture surface which indicate that failure was due to fatigue.Final fracture occurs when the crack has grown to a size where the stress intensity factor equals the fracture toughness K_{Ic} of the material. The crack propagates unstably throughout the specimen,

causing catastrophic fracture. The appearance of this part of the fracture surface differs from that created by fatigue crack growth. Macroscopically, the surface is jagged; microscopically, a dimple fracture surface, a brittle cleavage fracture, or a mixture of both types results, depending on the ductility of the material (Fig. 21 and Fig. 22).

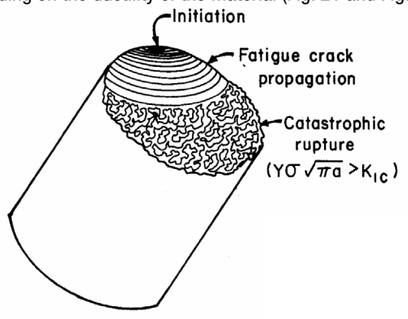

Fig. 21 Schematic drawing of the fatigue fracture surface of a circular shaft.

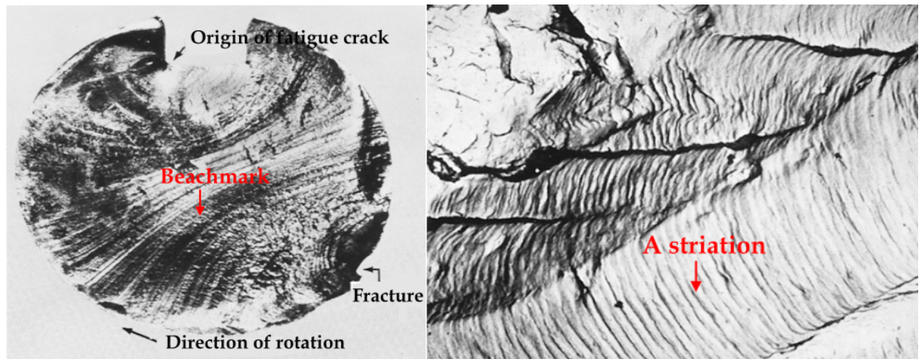

Fig. 22 Fatigue fracture surface of a steel shaft.

3.3 Fatigue life

Many factors, in addition to stress, strain, amplitude, etc., influence the fatigue life of materials. Here, the effects of (a) stress-based and (b) strain-based evaluations of fatigue life will be considered for low- and high-cycle cases. In the past, but also at present, the stress-based approach is quite common.

3.3.1 The stress-based approach

Various wave forms of cyclic stresses may be applied to a specimen for testing its suitability to act for a specific purpose in which good fatigue resistance is required. Fig. 23 is an illustration of stress cycles to which machine elements in industrial applications may be exposed. The first three illustrations in Fig. 23 represent sinusoidal-type cycles and the last one is a repeated cycle, possibly representing a specimen exposed to repeated stress. Airplanes and outer-space vehicles are not exposed to such regular stresses. Usually, the stresses acting, e.g., on the wings of airplanes, are irregular by nature.

Various types of machines are available on the market for applying any of the three usual types loading, namely, tension-

compression, torsion and flexure. The results of such tests are generally recorded as stress versus the number of cycles applied. The term for the resulting graphs, constructed from the recorded data of these tests, is 'S-N curves'. Fig.24 shows schematic S-N curves. In this approach, the fatigue life (number of cycles N) is related to the applied stress range ($\Delta\sigma$ or S) or the stress amplitude (σ_a). In general, a plot of the fatigue life versus the true stress amplitude for a metal gives a curve of the Basquin form:

$$\sigma_a = \frac{E.\Delta\varepsilon_e}{2} = \sigma_f^1.(2N)^b \qquad (1)$$

where N is the number of cycles to failure, 2N is the number of load reversals to failure, σ_f^1 is the fatigue strength coefficient, and b is the fatigue strength exponent (the sign of b is negative).

In a component or structure, there are two types of stress concentration. One is due to the structural geometry change or discontinuity, and the other is due to welding. Depending on how the stress concentration effect is accounted for, stress-based approaches can be further divided into the nominal stress approach, the hot-spot stress approach, and the notch stress approach. Currently, the hot-spot stress approach seems to be the one most favored by ship classification societies.

Metals and alloys showing a definite fatigue limit, such as the ferrous metals or titanium, are characterized by their ability to endure a large number of stress-cycles at the stress of the horizontal line and below it. The stress at this line is known as the 'endurance limit' (Fig. 25). In most of the non-ferrous metals, no definite limit exists and the number of cycles that they can endure without failure increases monotonically with decreased applied stress.

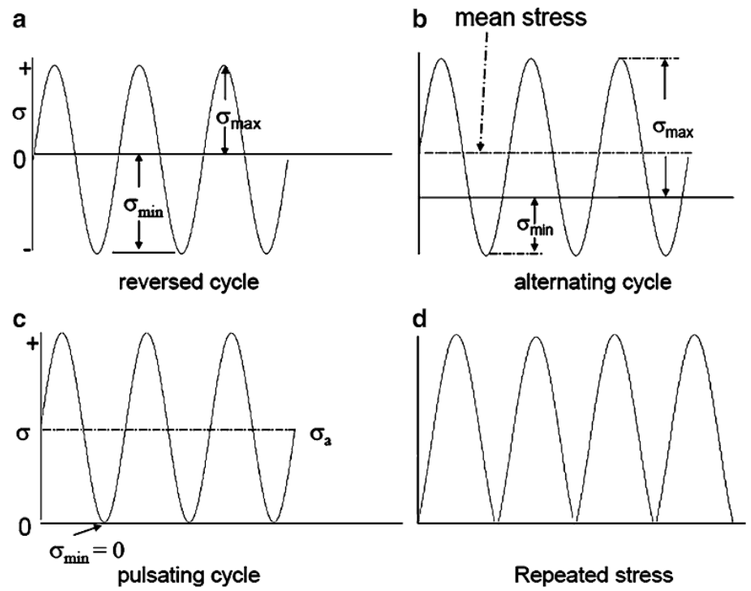

Fig. 23 Various forms of cyclic stresses: (a), (b) and(c) are sinusoidally varying cycles and (d) represents a repeating cycle

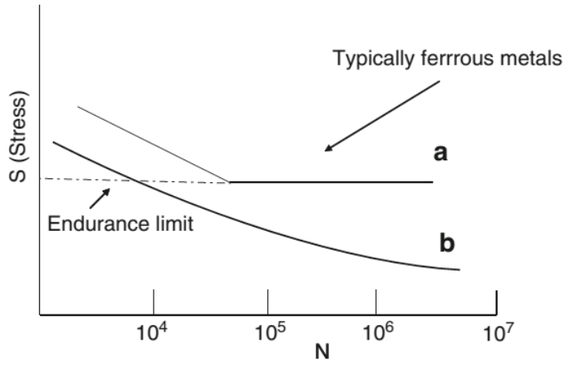

Fig. 24 S-N curves: (a) with a well-defined endurance limit and (b) without a definite fatigue limit.

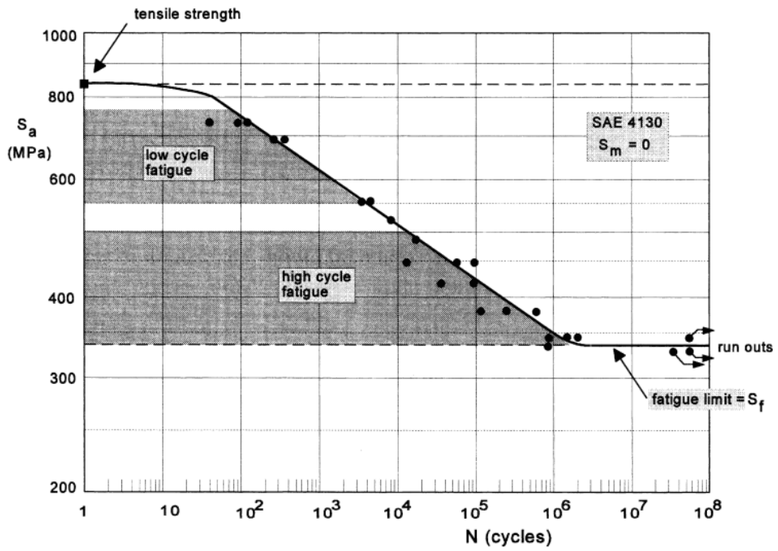

Fig. 25 Fatigue test results of unnotched specimens of a low-alloy steel (SAE 4130)

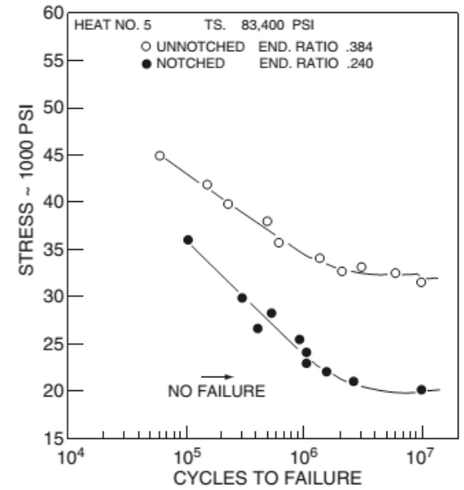

Fig. 26 S-N notched and unnotched specimens (Moore) are compared in the illustration. The endurance limit is indicated.

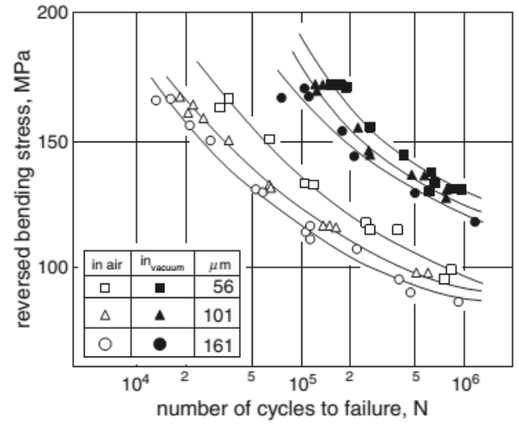

Fig. 27 S-N curves of Cu at different grain sizes in air and vacuum.

3.3.1.1 The endurance limit in ferrous metals

In Fig. 25, one of the S-N curves shows a sharply-defined knee, characterizing ferrous metals and a few others, such as Ti alloys. The endurance limit, or as it is often called, the 'fatigue limit', is typically parallel to the x-axis, which, as indicated in the above graph, represents the number of cycles-to-failure at a given stress. In theory, a material characterized by the endurance limit can perform at this stress level indefinitely (when the proper safety factors are taken into account) and can withstand in service a large number of cyclic stresses (as often stated as an infinite number). Fig. 26 shows experimental S-N curves for normalized and tempered Ni-Cr-Mo (8630) cast steel. Notched and unnotched specimens are compared in Fig. 26. One must realize that the allowable stress level decreases with increased cycles, so talk of a well-defined fatigue limit is meaningless (Fig. 27). The design of machine elements for operation over a very large number of cycles must not take for granted that any machine part will endure a certain stress for an unlimited number of cycles.

3.3.2 Strain-based life-times

In most practical cases of fatigue design, the critical location will be a notch in which plastic strains are imposed by surrounding elastic material. Thus, the situation will be strain-controlled, with a total strain range composed of an elastic

and a plastic part. The plastic strain resistance is best Strain-life fatigue analysis is more appropriate in low-cycle applications, where the applied strains have a significant plastic component, due to high load levels. The total amplitude of strain may be given as the sum of the elastic and plastic strains.

The plastic strain resistance is best described by the Manson–Coffin relationship.

$$\frac{\Delta\varepsilon_p}{2} = \varepsilon_f^1.(2N)^c \qquad (2)$$

where ε_f^1 is the fatigue ductility coefficient, and c is the fatigue ductility exponent (the sign of c is negative).

Manson and Hirschberg proposed that a metal's resistance to total-strain cycling can be considered as a superposition of its elastic and plastic strain resistance. By combining Eqs. 1 and 2.

$$\frac{\Delta\varepsilon_T}{2} = \varepsilon_a = \frac{\Delta\varepsilon_e}{2} + \frac{\Delta\varepsilon_p}{2} = \frac{\sigma_f^1}{E}(2N) + \varepsilon_f^1.(2N)^c \qquad (3)$$

The total-strain life curve approaches the plastic-strain life curve in the low cycle region and the stress life curve in the high cycle region. For general low-cycle and high-cycle fatigue, the Manson–Coffin relationship has a strong curvefit ability, but it needs to determine five material properties. Manson has simplified the equation even further with his method of universal slopes, where

$$\Delta\varepsilon = 3.5\ Su/E + (N)^{-0.1}\varepsilon + \varepsilon f^{0.6}\ (N)^{0.6} \qquad (4)$$

S_u, E, and ε_f are all obtained from a monotonic tensile test. He assumed that the two exponents are fixed for all materials, and that only S_u, E, and ε_f control the fatigue behavior.

3.3.3 Energy-based approach

A historical description of energy-based approaches is given by Fatemi and Yang. In using this type of failure criteria, it was realized that an energy-based damage parameter can unify the damage caused by different types of loading such as thermal cycling, creep, and fatigue. In conjunction with Glinka's rule, it is possible to analyze the damage accumulation of notched specimens or components by the energy approach.

Energy based damage models can also include mean stress and multi-axial loads, since multi-axial fatigue parameters based on strain energy have been developed.

Recently, the following fatigue strain energy density parameter for the critical plane to predict the fatigue life of various materials under multi-axial loading was proposed:

$$W^* = \Delta\sigma_{12}/2\ \ \Delta\gamma_{12}/2 + K_1\ K_2\ \ \Delta\varepsilon_{22}/2\ \ \Delta\sigma_{22}/2 \qquad (5)$$

where and are the shear and normal stress ranges in the critical plane, respectively, and are the shear and normal strain ranges in the critical plane, respectively, and k_1 and k_2 are two weight constants for strain and stress amplitudes, respectively, which are defined as:

$$k_1 = \gamma_f'/\varepsilon_f',\ k_2 = \sigma_f'/\tau_f' \qquad (6)$$

where is the uniaxial fatigue strength coefficient, and is the uniaxial fatigue ductility coefficient, is the torsional fatigue strength coefficient, and is the torsional fatigue ductility coefficient.

3.3.4 Continuum damage mechanics approaches

Continuum damage mechanics (CDM) is a relatively new subject in engineering mechanics and deals with the mechanical behavior of a deteriorating medium at the continuum scale. For the one-dimensional case,fatigue damage evolution per cycle can be generalized by a function of the load condition and damage state. By measuring the changes in tensile load-carrying capacity and using the effective stress concept, they formulated a nonlinear damage evolution equation as

$$D = 1 - [1 - r^{1/(1-\alpha)})]^{(1/(1+\beta)} \qquad (7)$$

where bis a material constant, ais a function of the stress state, and ris the damage state. This damage model is highly nonlinear in damage evolution, and is able to account for the mean stress effect. CDM models were mainly developed for

uniaxial fatigue loading. Some difficulties arise when these models are extended to multiaxial loading. Owing to the complexity of nonproportionalmultiaxial fatigue problems, a three-dimensional anisotropic CDM model does not yet exist. Great efforts are still needed to obtain an appropriate generalized prediction model for cumulative fatigue damage.

4. Conclusion

This article has briefly described the major microstructures and the phase transformations by which these microstructures are developed in carbon and low-alloy steels. Each type of microstructure and product is developed to characteristic property ranges by specific processing routes that control and exploit microstructural changes. The incorporation of steel carbon content into microstructure has a profound effect on microstructure and properties, and steels fall naturally into low-strength/high ductility/high toughness or high-strength/high fatigue resistant/low toughness groups with increasing carbon content. Metals are the most widely used materials in engineering structures, and one of the most common failure modes of metal structures is fatigue failure. Although metal fatigue has been studied for more than 160 years, many problems still remain unsolved. In this article, a state-of-the-art review of metal fatigue is carried out, with particular emphasis on the latest developments in fatigue life prediction methods. Fatigue prediction methods can only be evaluated if fatigue is understood as a crack initiation process followed by a crack growth period. The fatigue mechanism in metallic materials are basically associated with cyclic slip and the conversion into crack initiation and crack extension. Details of the mechanism are explained systematically.

5. References

ASM Handbook (1990). Properties and Selection: Irons, Steels, and High-Performance Alloys. volume1, ASM International.

Basquin, O.H. (1910). The exponential law of endurance tests, Proceedings of ASTM, Vol. 10(II), pp. 625-630.

Bennett, J.A. (1946). A study of the damaging effect of fatigue stressing on X4130 steel, Proceedings of ASTM, Vol. 46, pp. 693-714.

Callister William, D. (2003). Failure, In: Materials Science and Engineering: An Introduction, pp. 215-217, John Wiley and sons, Inc.

Campbell Glen, S. (1981). A note on fatal aircraft accidents involving metal fatigue, Int J Fatigue, Vol.3, pp. 181-185.

Chandler, H. (Ed.). (1994). Heat treater's guide: practices and procedures for irons and steels. ASM international.

Coffin Jr., L.F. (1954). A study of the effects of cyclic thermal stresses on a ductile metal, Trans. ASME, Vol. 76, pp. 931-950.

Corten, H.T.,Dolon, T.J. (1956). Cumulative fatigue damage, Proceedings of the International Conference on Fatigue of Metals, Institution of Mechanical Engineering and American Society of Mechanical Engineers, pp. 235-246.

Cui, W. (2002). A state-of-the-art review on fatigue life prediction methods for metal structures. Journal of marine science and technology, 7(1), 43-56.

Dowling N.E., Mean Stress Effects in Stress-Life and Strain-Life Fatigue. Society of Automotive Engineers, Inc., 2004, F2004/51

Fatemi A, Yang L (1998) Cumulative fatigue damage and life prediction theories: a survey of the state of the art for homogeneous materials. Int J Fatigue, Vol.20, pp. 9–34

Goodman J., Mechanics Applied to Engineering (Longmans Green, London, 1899).

Kommers, J.B. (1945). The effect of overstress in fatigue on the endurance limit of steel, Proceedings of ASTM, Vol. 45, pp. 532-541.

Krauss, G. (1989). Steels: heat treatment and processing principles. Materials Park: ASM international.

Manson, S.S. (1954). Behaviour of materials under conditions of thermal stress, NACA TN-2933, National Advisory Committee for Aeronautics.

Marco, S.M., Starkey, W.L. (1954). A concept of fatigue damage, Trans. ASME,Vol. 76, pp. 627-632.

Miner, M.A. (1945). Cumulative damage in fatigue, Journal of Applied Mechanics, Vol. 67, pp. A159-A164.

Palmgren, A. (1924). Die Lebensdauer von Kugellagern, Verfahrenstechinik, Berlin, Vol. 68, pp. 339-341.

Richart, F.E. and Newmark, N.M. (1948). An hypothesis for the determination of cumulative damage in fatigue, Proceedings of ASTM, Vol. 48, pp. 767-800.

Wohler, A. (1860). Versucheuber die Festigkeit der Eisenbahnwagenachsen, Zeitschrift fur Bauwesen,10; English summary (1867), Engineering, Vol.4, pp.160-161.